Helicopter Shaft Heating Parameters for Polyamide-11 Coating

Selim KEVRAN Ph.D
The Ministry of National Defence, dennssel@hotmail.com

Uğur ATİCİ
Assistant Professor, uatici@cumhuriyet.edu.tr

Most aviation parts are internationally supplied, with long lead times and high-cost spare parts. Spare parts with long lead times and high costs are very demanding in maintenance and repair and require advanced technical skills. Corrosion is a common mistake in maintenance and repair spare parts that are not made to appropriate standards. Corrosion reduces the life cycle of parts due to damage to the metal surface and internal structure and can cause irreversible fatal and material accidents. For this reason, one of the most effective methods that protect metal surfaces from corrosion is surface coating. Different coating processes such as electrolytic coating, thermal spray coating, electrolytic coating methods are applied to spare parts used in aircraft maintenance and repair operations. One of these coatings is polymeric powder coatings. Because polymeric powder coatings are environmentally friendly, they are applied instead of electrolytic coatings to special parts that should not contact acidic or alkaline chemicals. Polymers show thermoset and thermoplastic behavior under heat. Polymeric powder coatings are applied to the parts to be applied by electrostatic, thermal spray, and fluidized bed dipping methods. Although each method has its own advantages and disadvantages, the method to be applied is completely determined by the user's technical characteristics and the part. The homogeneous temperature distribution on the part surface after heating ensures that the coating thickness is equal on the entire surface. Determining the temperature distributions on metal parts' surfaces during heating is very difficult for parts with complex geometries (Koryagin et al., 2020). This study's motivation is to develop a new method that allows partial repairs of high-cost main structural spare parts with a long lead time and complex geometries.

This study consists of five sections. Relevant past studies are presented in the second section, problem definition, experimental design and heating mechanism in the third section, thermal analysis and the results obtained from thermal analysis in the fourth section, and the conclusion and future work are presented in the fifth section.

Literature Review

Today, environmental alternatives instead of petroleum-based composites are widely investigated. One of these alternatives is polyamide-11 (PA11). PA11-based composites can be used instead of glass fiber, and lignocellulose fiber composite reinforced types are environmentally sustainable (Oliver-Ortega et al., 2018). The thermal conductivity of coatings varies depending on the porosity level (Yugeswaran et al., 2021). Coatings have advantages or disadvantages depending on the area of use. Tool coatings with a high friction coefficient create a build-up edge between the tool and the work piece and increase the cutting temperature (Li, Lü et al., 2021). Composite coatings improve the performance of alloys (Zhang et al., 2021). Low porosity tungsten coatings exhibit a high bond strength to copper

substrates and accumulate pressure stresses (Rybin et al., 2021). Also, coating thickness affects electrical conductivity (Hung et al., 2021).

In aviation, PA11 coatings attract attention due to environmental concerns and corrosion resistance. Coating spare parts used in aircraft manufacturing and maintenance operations against crozant is essential for main structural parts such as shaft and tail drive shaft. These types of structural parts are subject to rigorous technical specifications (Li et al., 2012). Damage-resistant methodologies are used for spare parts subjected to high-frequency repetitive loads (Fossati et al., 2020). Since the shaft and rotor stresses are important for flight safety, the bending stresses acting on the main rotor shaft of a single rotor helicopter are monitored (Nedelko et al., 2019). Structural resonance causes wear on gear wheels. If this type of wear is examined in time and the spare part is not replaced with a new one, it may cause the aircraft accident (Gębura et al., 2019). Cracks and resonance are the main parameters that affect the aircraft, and such parameters are carefully controlled in terms of flight safety. The signal generated by the crack is used to monitor cracked shafts based on vibration (Girondin et al., 2015). The helicopter shaft is one of the high-speed spare parts, and it affects the aircraft performance depending on the assembly method (Yeo, 2019). The chords' position on the blade can be expressed as another parameter that affects the performance of the aircraft and flight safety (Han et al., 2018). Main structures such as shaft, main gearbox, and rotor are followed through monitoring programs to ensure the aircraft's integrity (Zhou et al., 2018). Shaft, rotor, and shaft bearings must be monitored for aircraft safety (Zhou et al., 2019). Aircraft safety affects not only its components but also environmental factors. Foreign matter damage causes plastic deformation and causes aviation accidents (Infante & Freitas, 2019).

In recent years, designs using carbon fiber composite materials in power transmission systems have developed (Henry & Mills, 2019). All spare parts on the aircraft affect flight safety. Aircraft coupling and energy transfer relations should be considered in flight conditions (Li & Xuan, 2017). Vibration-based methods are used to detect early malfunction of spare parts used for power transmission in helicopters during flight (Camerini et al., 2018). Risk assessment techniques are used to determine failure modes in lubrication systems (Rashid et al., 2015). Heat treatment affects the hardness and torsion values of spare parts such as intermediate gear, drive fan (Manda et al., 2018).

Many parameters affect the quality of the coating process. It is important to determine the parameters according to the problem being investigated. Taguchi method is widely used in determining the optimum values of experimental parameters in the literature (Kazemian et al., 2021). In the Taguchi method, factors affecting the experiment and the levels of these factors are determined. Although the factors are specific to the problem under investigation, parameters such as feed input, speed, temperature, and altitude can be mentioned as examples (Ye et al.,

2021). The levels corresponding to the factors are determined again depending on the experimental parameters (Li, Wang, et al., 2021). Many researchers have used the Taguchi method to determine the optimum experimental parameters. Taguchi method is used in the determination of heat exchanger performance (Biçer et al., 2020), the inspection of micro-channel heat sink thermal materials (Naqiuddin et al., 2018).

Besides that, the Taguchi method has been used in the manufacturing sector and in determining the parameters affecting the coating. Determination of optimum curing parameters (Teng & Hwang, 2007), determination of heat treatment conditions (Leisk & Saigal, 1995), choice of coating material (Özel et al., 2020), application of carbon coating on piston rings (Tyagi et al., 2020), determination of conditions of electroless Ni-P (EN) coating (Park & Kim, 2019), calculation of optimal coating thickness LPCS (Winnicki et al., 2014), the effect of sliding speed and texture density on friction (Segu et al., 2013), determination of automation parameters in microcontroller coating (Ramesh Kumar et al., 2020) determination of automation parameters in microcontroller coating (Park et al., 2021) determination of optimal turning control parameters (Dutta & Kumar Reddy Narala, 2021; Singh & Sultan, 2019) and determination of optimum cutting conditions (Chethan et al., 2019) can be given as an example to these studies.

Material and Method

The driving force for heat transfer during the heating process is the temperature difference. Temperature is the average kinetic energy value of the molecules forming the part. Heat is the energy transferred from a hot part to a lower temperature part. Heat transfer continues until the temperatures of the parts are equal to each other. Heat transfer occurs through three different methods: conduction, convection, and radiation.

In heat transfer with Fourier conduction, the amount of heat passing through the unit area perpendicular to the heat flow is directly proportional to the temperature gradient in the heat flow direction. q heat quantity W, A heat transfer area m2, k heat conduction coefficient (W/mK), $\frac{dT}{dx}$ (K/m) to be the temperature gradient in the heat flow direction. The specific heat transfer coefficient of the material is presented in Eq.1.

$$Energy_{input} - Energy_{output} = \frac{\partial E}{\partial t} \tag{1}$$

According to the energy conservation law, the energy conservation of a control volume is presented in Eq.2 for cylindrical coordinates.

$$\frac{1}{r}\frac{\partial}{\partial r}\left(kr\frac{\partial T}{\partial r}\right) + \frac{1}{r^2}\frac{\partial}{\partial \emptyset}\left(k\frac{\partial T}{\partial \emptyset}\right) + \frac{\partial}{\partial z}\left(k\frac{\partial T}{\partial z}\right) + q = \rho c_p \frac{\partial T}{\partial t} \tag{2}$$

The temperature distribution of a cylindrical shaft changes in the radial direction. If it is assumed that the shaft is isotropic and the heat transfer coefficient is constant, the transient state heat equation giving the temperature change along the radial direction is presented in Eq.3 since there is no heat generation on the heat transfer surface.

$$\frac{1}{r}\frac{\partial}{\partial r}\left(kr\frac{\partial T}{\partial r}\right) = \frac{\rho c_p}{k}\frac{\partial T}{\partial t} \tag{3}$$

Here ρ denotes the density value, c_p denotes the specific heat value, $\frac{\rho c_p}{k}$ value is also referred to as $\frac{1}{\alpha}$. α indicates the thermal diffusivity value specific to the substance. Besides, an equation showing the heat transfer by convection from the furnace's inner environment to the shaft surface at any time and known as the Newton Cooling Equivalence is presented in Eq.4.

$$Q \text{ convection} = hA_s(T_f - T_s)\partial T \tag{4}$$

h indicates the convection heat transfer coefficient of the air inside the furnace (W/m^2K), A indicates the surface area of the part (m^2), T_f the furnace temperature (K) and T_s the surface temperature (K) of the part. This amount of heat transferred by convection is equal to the increase in the shaft's internal energy, where m is the mass (g) of the part, c_p is the specific heat (J/gK), and ∂T is the temperature change (K) (Eq.5). Since the heat flowing in the furnace by convection is equal to the increase in the part's internal energy, Eq.6 is obtained. By substituting ρV for m and integrating the part surface temperature at time $t = 0$ with the condition that T_s (i) and the part temperature at any time t with the condition that T_s (t), the equation gives the particle temperature at any time t is obtained.

$$Q = mc_p\partial T \tag{5}$$
$$mc_p\partial T = hA_s(T_f - T_s)\partial T \tag{6}$$

Problem Definition

In this study, the heating parameters for PA11 coating of the shaft's gear surface without changing the torsion property of the helicopter shaft were investigated. PA11 coating curing time depends on the amount of heat applied. Curing temperature and times are presented in Figure 1.

The helicopter's instant engine speed is measured by the torsion angle formed in the middle of the shaft with the applied power. However, the temperature value of the shaft torsion measurement zone during curing should be $80 \pm 10°C$ (Airbus, 2014). The temperature limit value required for curing (minimum 260 C for 35-90 minutes) is above the temperature limits (80 ± 10 °C) for the torsion zone. Heating affects the torsion angle value. To not change the twisting property of the shaft, the entire shaft cannot be placed in the furnace during curing. PA11 coating surface and torsion measurement area on the shaft are presented in Figure 2.
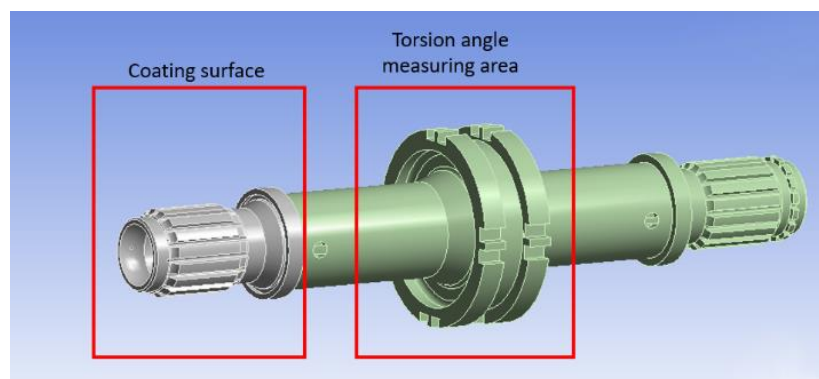
Figure 1

PA11 Coating Curing Temperature and Time Graph(Arkema)

Figure 2

Coating Surface and Torsion Angle Measurement Area

Since the entire shaft cannot be placed inside the furnace, a new heating mechanism has been designed for heat treatment since the furnace door cannot be heated openly. The heating device consists of a new cover that allows only the shaft

coating surface to be inserted into the furnace and a support element for the part of the shaft remaining outside the furnace. The designed heating setup is presented in Figure 3.

Figure 3
Designed Heating Setup

Experimental Design

To monitor the heat change in the region to be coated and the heat change in the torsion region, K-type probes were placed in the middle part of the shaft inside the furnace. Temperature values were recorded during the heating process.

PA11 coating quality depends on the type of furnace preheating, the heating time, and temperature. Taguchi method was used to determine heating parameters before coating. Taguchi is a statistical method developed for quality improvement in the industry. It aims to see the different factors to be investigated and the relationships of these factors with the least experimentation and statistically estimating them. The airflow coefficient for the oven can be changed by using a fan. Experiments In two different furnaces, without fan ($T1$) and with the fan ($T2$) oven interior temperature 290 °C, 300 °C, and 330 °C, heating time 1800, 2700, and 5400 seconds, coating surface temperature (CST) and torsion area after heating. The temperature (TZT) orthogonal matrix is presented in Table 1.

Table 1

Orthogonal Matrix

HTC	Time	Temperature	CST	TMA
T1	1800	290	135.0	54.5
T1	1800	300	155.0	63.4
T1	1800	330	175.0	75.1
T1	2700	290	150.0	54.5
T1	2700	300	165.0	63.4
T1	2700	330	185.0	75.1
T1	5400	290	140.0	63.4
T1	5400	300	172.0	75.6
T1	5400	330	193.7	85.0
T2	1800	290	145.0	72.0
T2	1800	300	165.0	79.0
T2	1800	330	185.0	84.0
T2	2700	290	267.3	70.0
T2	2700	300	282.0	75.0
T2	2700	330	285.2	80.0
T2	5400	290	267.0	75.0
T2	5400	300	283.0	80.0
T2	5400	330	293.0	85.0

The smallest signal/noise ratio techniques were used to determine the coating surface temperature. Its graphic is presented in Figure 4. According to the temperature change in the coating surface, the furnace type is determined as T2. The duration is 5400 seconds, and the furnace's temperature is 330 ° C.

Figure 4

Signal/Noise Graph of Coating Surface Temperature Change
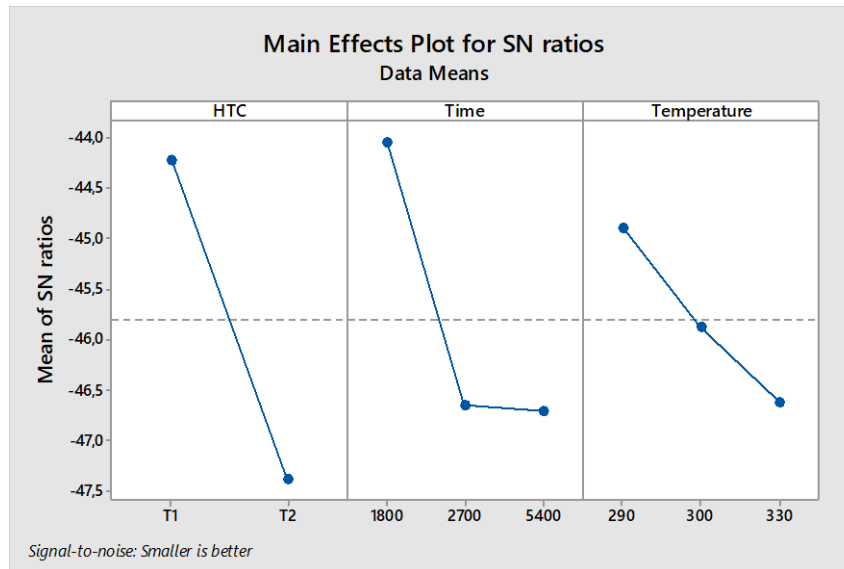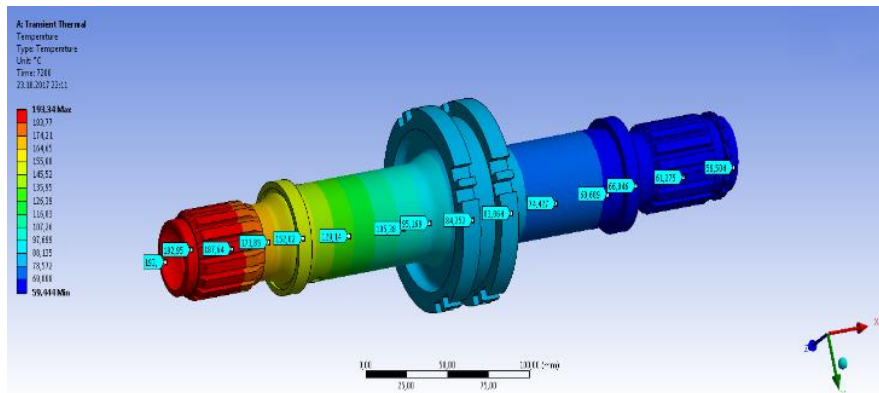

Findings

This study's experimental temperature data were obtained with a K-type probe connected to the shaft coating surface inside the furnace and the middle part of the shaft outside the furnace. In a fanless (T1) and fanned (T2) furnace, the shaft's thermal analysis to be coated, and the area outside the furnace was performed. Surface temperatures of the shaft outside and inside the oven during the 5400 seconds minutes heating process are presented in Table 2.

The part of the shaft outside the furnace is heated by conduction and also loses its heat by convection due to room conditions. The ratio of heat flux transferred to the temperature gradient in conduction heat transfer is constant. With the existing preheating parameters, it was determined that the thermal value required for curing the surface of the shaft to be coated was not reached in the oven without a fan. With the current parameters and the way of heating, it has been determined that the area of the shaft that is desired to be coated can reach 193 °C at most. The temperature distribution obtained at the end of the thermal analysis is presented in Figure 5.

Table 2

Thermal Analysis Result of the Shaft

| Furnace type	T1		T2	
Time [sec]	Torsion area Temp.[°C]	Coating surface Temp .[°C]	Torsion area Temp. [°C]	Coating surface Temp. [°C]
72	22	40	25	52
144	26	78	33	89
360	33	112	43	127
720	46	138	53	192
1440	60	159	66	245
1800	67	167	74	259
2400	72	175	83	278
2700	75	178	87	285
3200	79	181	96	287
3600	81	182	102	289
4500	83	187	110	291
5400	84	193	115	293

Figure 5

Shaft Surface Temperature Distribution

It was observed that the highest temperature value measured experimentally was at most 186 ℃ at the end of the whole heating process. It has been determined from both the thermal analysis made with the ANSYS program and the experimental measurements that the shaft area to be coated with the existing furnace cannot be heated to 280 ℃ required for polyamide coating application.

The heating process was carried out by using optimum experimental parameters obtained by the Taguchi method. The surface temperatures outside and

inside the furnace, connected to the shaft surface inside the furnace and the middle part of the shaft outside the furnace, were recorded.

The torsion area temperature for 2000 seconds to 5400 seconds between the target temperature values (80 ± 10 ℃) in the fanless type oven. The coating zone temperature reached 193 C at the end of 5400 seconds. The torsion zone temperature for 1700 seconds to 3000 seconds between the target temperature values (80 ± 10 ℃) in the fan-type oven. The coating zone temperature reached 280 ± 10 ℃ at the end of 2300 seconds. The fanless (T1) and fanned (T2) furnace, the coating surface, and the torsion measurement area, heat change graphs are presented in Figure 6.

Figure 6
Shaft Heat Change Graph in the Funned & Fanless Furnace

—Torsion measurement area (°C)　　—Coating surface temperature (°C)
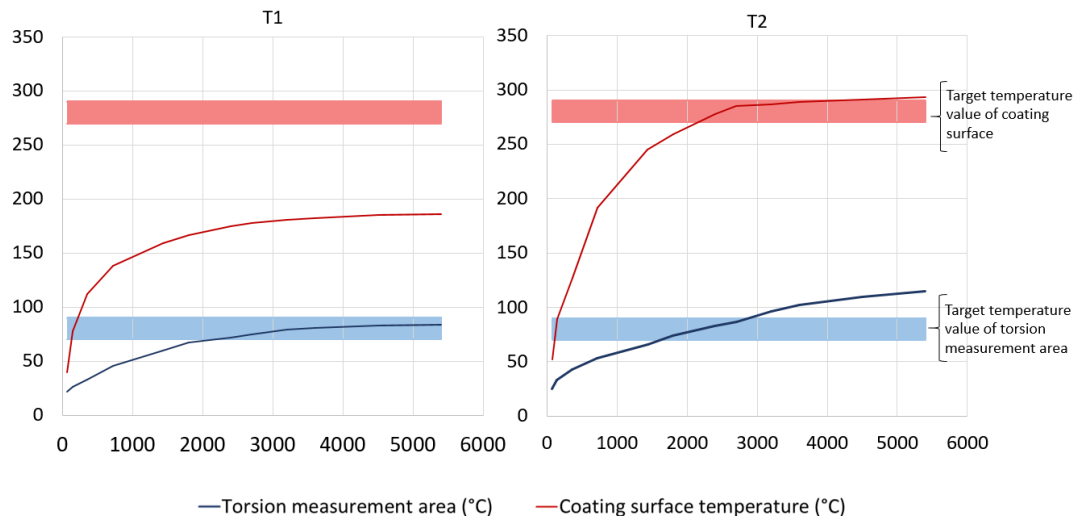
According to the ANSYS program's thermal analysis, it has been determined that the targeted temperature can be reached at a temperature of 330 ℃ with a fan (heat transfer coefficient of 40 W/m^2K) and air circulation inside the oven. As a result of the thermal analysis, it was determined that the shaft reached 285 ℃ at the end of 2700 seconds and 293 ℃ at the end of 7200 seconds. According to the termal analysis, optimum heating parameters of PA11 coating (coating surface, the furnace type and initial furnace temperature) are determined as T2 (40 W/m^2K), 2700 and 330 ° C. Thermal analysis of the shaft with optimum test parameters are presented in Figure 7.

Figure 7

Thermal Analysis of the Shaft with Determined Test Parameters
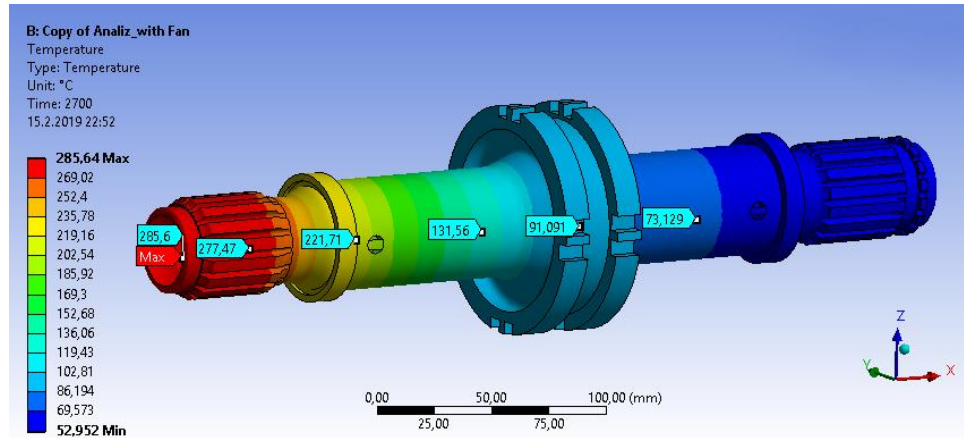
CONCLUSION

In this study, the heating parameters that should be applied for the PA11 coating of the helicopter shaft were investigated. The helicopter's abrupt engine speed is measured by the torsion angle formed in the middle of the shaft with the applied power. The torsion measurement area temperature can be a maximum of 80 ± 10 °C during the heat treatment-otherwise, the shaft changes' torsional property. For the PA11 coating to cure, it should be 280 ± 10 °C, depending on the heating time of the surface. A new heating system has been designed for the coating of the helicopter shaft with PA11. Thus, the heating process could be performed while the coating surface was inside the oven. The torsion measurement zone was outside of the oven. To monitor the temperature change in the region to be coated and the temperature change in the torsion region, K-type probes were placed in the middle part of the shaft inside the oven. The temperature values were recorded. Taguchi method was used to determine heating parameters before coating. According to the smallest signal/noise ratio technique, the furnace type was determined as T2 in the experimental parameters. The duration was 2700 seconds, and the furnace temperature was 330 °C. It has been determined that the coating surface of the shaft in the T1 furnace can reach a maximum of 193 °C with the current parameters and heating method.

In the heating process in the fanless type oven for 5400 seconds, the torsion area temperature is between the targeted temperature values (80 ± 10 °C). The coating zone temperature reached 193 °C at the end of 5400 seconds. The torsion zone temperature up to 3000 seconds in the fan-type oven is between the target

temperature values (80 ± 10 ℃). The coating zone temperature reached 280 ± 10 ℃ at the end of 2300 seconds.

It has been determined from the thermal analysis made with the ANSYS program that the targeted temperature can be reached at a temperature of 330 ℃ with a fan oven with a coefficient of heat transfer coefficient of $40\ W/m^2K$ and air circulation inside the oven. As a result of thermal analysis, the shaft's coating surface temperature is 285 ℃ at the end of 2700 seconds, and the torsion zone temperature is between the targeted temperature values (80 ± 10 ℃). In the experiment conducted, it was understood from the thermal analysis performed with the ANSYS program that the convection heat transfer in a fan oven is much more efficient than the convection heat transfer with a fanless oven.

References

Airbus. (2014). *AS 532 maintenance manual*. Airbus.com

Arkema. (2021). *Innovative and sustainable solutions products*. https://www.arkema.com/global/en/products/

Biçer, N., Engin, T., Yaşar, H., Büyükkaya, E., Aydın, A., & Topuz, A. (2020). Design optimization of a shell-and-tube heat exchanger with novel three-zonal baffle by using CFD and taguchi method. *International Journal of Thermal Sciences, 155*, 106417. doi:https://doi.org/10.1016/j.ijthermalsci.2020.106417

Camerini, V., Coppotelli, G., & Bendisch, S. (2018). Fault detection in operating helicopter drivetrain components based on support vector data description. *Aerospace Science and Technology, 73*, 48-60. doi:https://doi.org/10.1016/j.ast.2017.11.043

Chethan, Y. D., Ravindra, H. V., & Krishnegowda, Y. T. (2019). Optimization of machining parameters in turning Nimonic-75 using machine vision and acoustic emission signals by Taguchi technique. *Measurement, 144*, 144-154. doi:https://doi.org/10.1016/j.measurement.2019.05.035

Dutta, S., & Kumar Reddy Narala, S. (2021). Optimizing turning parameters in the machining of AM alloy using Taguchi methodology. *Measurement, 169*, 108340. doi:https://doi.org/10.1016/j.measurement.2020.108340

Fossati, M., Pagani, M., Giglio, M., & Manes, A. (2020). Fatigue crack propagation in a helicopter component subjected to impact damage. *Defence Technology*. doi:https://doi.org/10.1016/j.dt.2020.02.005

Gębura, A., Kłysz, S., & Tokarski, T. (2019). Monitoring wear of gear wheel of helicopter transmission using the FAM-C and FDM-A methods. *Procedia Structural Integrity, 16,* 184-191. doi:https://doi.org/10.1016/j.prostr.2019.07.039

Girondin, V., Morel, H., Cassar, J.-P., & Pekpe, K. M. (2015). Vibration-based fault detection of meshing shafts. *IFAC-PapersOnLine, 48*(21), 560-565. doi:https://doi.org/10.1016/j.ifacol.2015.09.585

Han, D., Yang, K., & Barakos, G. N. (2018). Extendable chord for improved helicopter rotor performance. *Aerospace Science and Technology, 80*, 445-451. doi:https://doi.org/10.1016/j.ast.2018.07.031

Henry, T. C., & Mills, B. T. (2019). Optimized design for projectile impact survivability of a carbon fiber composite drive shaft. *Composite Structures, 207*, 438-445. doi:https://doi.org/10.1016/j.compstruct.2018.09.049

Hung, S.-M., Lin, H., Chen, H.-W., Chen, S.-Y., & Lin, C.-S. (2021). Corrosion resistance and electrical contact resistance of a thin permanganate conversion coating on dual-phase LZ91 Mg-Li alloy. *Journal of Materials Research and Technology*. doi:https://doi.org/10.1016/j.jmrt.2021.02.050

Infante, V., & Freitas, M. (2019). Failure analysis of compressor blades of a helicopter engine. *Engineering Failure Analysis, 104*, 67-74. doi:https://doi.org/10.1016/j.engfailanal.2019.05.024

Kazemian, A., Parcheforosh, A., Salari, A., & Ma, T. (2021). Optimization of a novel photovoltaic thermal module in series with a solar collector using Taguchi based grey relational analysis. *Solar Energy, 215*, 492-507. doi:https://doi.org/10.1016/j.solener.2021.01.006

Koryagin, S. I., Velikanov, N. L., & Sharkov, O. V. (2020). Effect of polymer coating on stress concentration of sheet element with a hole. *Materials Today: Proceedings*. doi:https://doi.org/10.1016/j.matpr.2020.08.112

Leisk, G., & Saigal, A. (1995). Taguchi analysis of heat treatment variables on the mechanical behavior of alumina/aluminum metal matrix composites. *Composites Engineering, 5*(2), 129-142. doi:https://doi.org/10.1016/0961-9526(95)90709-K

Li, C., Guan, Y., Feng, Y., Jiang, C., Zhen, S., & Su, X. (2021). Comparison of influencing factors and level optimization for heating through deep-buried pipe based on Taguchi method. *Geothermics, 91*, 102045. doi:https://doi.org/10.1016/j.geothermics.2021.102045

Li, G., Lü, W., Liu, S., Li, C., Zhou, Y., & Wang, Q. (2021). Multilayer-growth of TiAlN/WS self-lubricating composite coatings with high adhesion and their cutting performance on titanium alloy. *Composites Part B: Engineering, 211*, 108620. doi:https://doi.org/10.1016/j.compositesb.2021.108620

Li, H. C. H., Wang, J., & Baker, A. (2012). Rapid composite bonded repair for helicopter tail drive shafts. *Composites Part B: Engineering, 43*(3), 1579-1585. doi:https://doi.org/10.1016/j.compositesb.2011.08.012

Li, Y., & Xuan, Y. (2017). Thermal characteristics of helicopters based on integrated fuselage structure/engine model. *International Journal of Heat and Mass Transfer, 115*, 102-114. doi:https://doi.org/10.1016/j.ijheatmasstransfer.2017.07.038

Manda, P., Sambasiva Rao, A., Singh, S., & Singh, A. K. (2018). Failure analysis of cooler fan drive gear system of main gear box of helicopter. *Materials Today: Proceedings, 5*(9, Part 3), 17737-17745. doi:https://doi.org/10.1016/j.matpr.2018.06.097

Naqiuddin, N. H., Saw, L. H., Yew, M. C., Yusof, F., Poon, H. M., Cai, Z., & Thiam, H. S. (2018). Numerical investigation for optimizing segmented micro-channel heat sink by Taguchi-Grey method. *Applied Energy, 222*, 437-450. doi:https://doi.org/10.1016/j.apenergy.2018.03.186

Nedelko, D., Urbahs, A., Turko, V., Urbaha, M., Carjova, K., & Nagaraj, P. (2019). Assessment of the limits of signs of health and usage monitoring

system for helicopter transmission. *Procedia Computer Science, 149*, 252-257. doi:https://doi.org/10.1016/j.procs.2019.01.131

Oliver-Ortega, H., Llop, M. F., Espinach, F. X., Tarrés, Q., Ardanuy, M., & Mutjé, P. (2018). Study of the flexural modulus of lignocellulosic fibers reinforced bio-based polyamide11 green composites. *Composites Part B: Engineering, 152*, 126-132. doi:https://doi.org/10.1016/j.compositesb.2018.07.001

Özel, S., Vural, E., & Binici, M. (2020). Optimization of the effect of thermal barrier coating (TBC) on diesel engine performance by Taguchi method. *Fuel, 263*, 116537. doi:https://doi.org/10.1016/j.fuel.2019.116537

Park, I.-C., & Kim, S.-J. (2019). Cavitation erosion behavior in seawater of electroless Ni-P coating and process optimization using Taguchi method. *Applied Surface Science, 477*, 37-43. doi:https://doi.org/10.1016/j.apsusc.2018.02.033

Park, S., Chuang, H.-S., & Kwon, J.-S. (2021). Numerical study and Taguchi optimization of fluid mixing by a microheater-modulated alternating current electrothermal flow in a Y-shape microchannel. *Sensors and Actuators B: Chemical, 329*, 129242. doi:https://doi.org/10.1016/j.snb.2020.129242

Ramesh Kumar, R., Rajalakshmy, P., Saranya, M. D., Kirubakaran, S., Granty Regina Elwin, J., & Marichamy, S. (2020). Process automation through internet of things on copper coating process of stainless steel. *Materials Today: Proceedings*. doi:https://doi.org/10.1016/j.matpr.2020.10.701

Rashid, H. S. J., Place, C. S., Mba, D., Keong, R. L. C., Healey, A., Kleine-Beek, W., & Romano, M. (2015). Reliability model for helicopter main gearbox lubrication system using influence diagrams. *Reliability Engineering & System Safety, 139*, 50-57. doi:https://doi.org/10.1016/j.ress.2015.01.021

Rybin, D. K., Batraev, I. S., Dudina, D. V., Ukhina, A. V., & Ulianitsky, V. Y. (2021). Deposition of tungsten coatings by detonation spraying. *Surface and Coatings Technology, 409*, 126943. doi:https://doi.org/10.1016/j.surfcoat.2021.126943

Segu, D. Z., Kim, J.-H., Choi, S. G., Jung, Y.-S., & Kim, S.-S. (2013). Application of Taguchi techniques to study friction and wear properties of MoS2 coatings deposited on laser textured surface. *Surface and Coatings Technology, 232*, 504-514. doi:https://doi.org/10.1016/j.surfcoat.2013.06.009

Singh, K., & Sultan, I. (2019). Parameters optimization for sustainable machining by using Taguchi method. *Materials Today: Proceedings, 18*, 4217-4226. doi: https://doi.org/10.1016/j.matpr.2019.07.380

Teng, S.-Y., & Hwang, S.-J. (2007). Predicting the process induced warpage of electronic packages using the P–V–T–C equation and the Taguchi method.

Microelectronics Reliability, 47(12), 2231-2241. doi:https://doi.org/10.1016/j.microrel.2007.01.084

Tyagi, A., Pandey, S. M., Murtaza, Q., Walia, R. S., & Tyagi, M. (2020). Tribological behavior of carbon coating for piston ring applications using Taguchi approach. *Materials Today: Proceedings, 25*, 759-764. doi:https://doi.org/10.1016/j.matpr.2019.09.004

Winnicki, M., Małachowska, A., & Ambroziak, A. (2014). Taguchi optimization of the thickness of a coating deposited by LPCS. *Archives of Civil and Mechanical Engineering, 14*(4), 561-568. doi:https://doi.org/10.1016/j.acme.2014.04.006

Ye, X., Kang, Y., Chen, B., Deng, S., Yan, Z., & Zhong, K. (2021). Study of multi-objective optimization of overall ventilation performance for an impinging jet ventilation system using Taguchi-based grey relational analysis. *Building and Environment, 188*, 107431. doi:https://doi.org/10.1016/j.buildenv.2020.107431

Yeo, H. (2019). Design and aeromechanics investigation of compound helicopters. *Aerospace Science and Technology, 88*, 158-173. doi:https://doi.org/10.1016/j.ast.2019.03.010

Yugeswaran, S., Amarnath, P., Ananthapadmanabhan, P. V., Pershin, L., Mostaghimi, J., Chandra, S., & Coyle, T. W. (2021). Thermal conductivity and oxidation behavior of porous Inconel 625 coating interface prepared by dual-injection plasma spraying. *Surface and Coatings Technology,* 126990. doi:https://doi.org/10.1016/j.surfcoat.2021.126990

Zhang, H. D., Chen, A. Y., Gan, B., Jiang, H., & Gu, L. J. (2021). Corrosion protection investigations of carbon dots and polydopamine composite coating on magnesium alloy. *Journal of Magnesium and Alloys*. doi:https://doi.org/10.1016/j.jma.2020.11.021

Zhou, L., Duan, F., Corsar, M., Elasha, F., & Mba, D. (2019). A study on helicopter main gearbox planetary bearing fault diagnosis. *Applied Acoustics, 147,* 4-14. doi:https://doi.org/10.1016/j.apacoust.2017.12.004

Zhou, L., Duan, F., Mba, D., Wang, W., & Ojolo, S. (2018). Using frequency domain analysis techniques for diagnosis of planetary bearing defect in a CH-46E helicopter aft gearbox. *Engineering Failure Analysis, 92*, 71-83. doi:https://doi.org/10.1016/j.engfailanal.2018.04.051